

GALEX OBSERVATIONS OF THE UV SURFACE BRIGHTNESS AND COLOR PROFILES OF THE LOCAL GROUP ELLIPTICAL GALAXY M32 (NGC221)

ARMANDO GIL DE PAZ¹, BARRY F. MADORE¹, YOUNG-JONG SOHN², YOUNG-WOOK LEE², MARK SEIBERT³, R. MICHAEL RICH⁴, LUCIANA BIANCHI⁵, TOM A. BARLOW³, YOUNG-IK BYUN², JOSÉ DONAS⁶, KARL FORSTER³, PETER G. FRIEDMAN³, TIMOTHY M. HECKMAN⁷, PATRICK JELINSKY⁸, ROGER F. MALINA⁶, D. CHRISTOPHER MARTIN³, BRUNO MILLIARD⁶, PATRICK MORRISSEY³, SUSAN G. NEFF⁹, DAVID SCHIMINOVICH³, OSWALD H. W. SIEGMUND⁸, TODD SMALL³, ALEX S. SZALAY⁷, BARRY Y. WELSH⁸, TED K. WYDER³

Submitted to ApJL

ABSTRACT

M32, the compact elliptical-galaxy companion to the Andromeda spiral galaxy has been imaged by the Galaxy Evolution Explorer (GALEX) in two ultraviolet bands, centered at ~ 1500 (FUV) and 2300 \AA (NUV). The imaging data have been carefully decomposed so as to properly account for the complicated background contamination from the disk of M31. We have derived the surface brightness and color profiles finding a slightly positive color gradient of $\Delta(FUV-B)/\Delta \log(r) = +0.15 \pm 0.03$ within one effective radius. Earlier data from the Ultraviolet Imaging Telescope suggested that M32 had an extremely large (negative) FUV-optical color gradient ($\Delta(FUV-B)/\Delta \log(r) < -2$), inverted with respect to the majority of gradients seen in giant elliptical galaxies. Our new results show that, despite of its very low UV-upturn, M32 has similar UV properties to those observed in luminous elliptical galaxies.

Subject headings: galaxies: elliptical and lenticular, fundamental parameters (colors), individual (M32), Local Group—ultraviolet: galaxies

1. INTRODUCTION

The compact elliptical galaxy M32 has been widely used in the past as template for the study of stellar populations and chemical evolution of elliptical galaxies (e.g. Freedman 1992 and references therein). It is very nearby (780 kpc; Tonry 1991; Freedman & Madore 1990). It has very high surface brightness at optical wavelengths and it is of high metallicity ($-0.2 < [\text{Fe}/\text{H}] < +0.01$; Grillmair et al. 1996).

However, the initial study of the UV properties of this galaxy by O’Connell et al. (1992) and more recently by Ohl et al. (1998) cast some doubt on M32 as being a truly typical example of an elliptical galaxy. These authors, using data from the Shuttle-borne Ultraviolet Imaging Telescope (UIT), claimed the presence of a strong FUV-optical color gradient in M32, but inverted with respect to the gradients observed in the vast majority of elliptical galaxies. While in regular, luminous elliptical galaxies the inner regions are slightly bluer than the outer parts (probably suggesting a stronger UV-upturn in the nuclear regions), for M32 these authors reported the opposite: a very strong blue trend (~ 3 mag within the effective radius; r_{eff}) toward outer regions of the galaxy.

Newly obtained GALEX FUV observations now show

that the FUV-optical gradient in M32 ($\Delta(FUV-B)/\Delta \log(r) = +0.15 \pm 0.03$) is in fact very similar to the gradients commonly measured in luminous elliptical galaxies. This analysis rests on a careful subtraction of the background emission from the disk of M31 (see e.g. Choi, Guhathakurta, & Johnston 2002). We suggest that the strong negative gradient reported by Ohl et al. (1998) may have been caused by problems in the density-to-flux calibration of UIT photographic data at low surface-brightness levels.

2. OBSERVATIONS

GALEX has recently completed a mosaic image of the entire Andromeda galaxy. This mosaic includes observations of the compact elliptical galaxy M32 with exposure times of 6138 seconds in the FUV band ($\lambda = 1530 \text{ \AA}$) and 4808 seconds in the NUV band ($\lambda = 2310 \text{ \AA}$). The final spatial resolution (FWHM) of the combined images of M32 used in this Letter was $6.0''$ and $6.8''$ for the FUV and for the NUV. The images were flux calibrated using the GALEX zero points (Morrissey et al. 2004).

In Figures 1a & 1b we show a $25' \times 25'$ section of the GALEX FUV and NUV images centered on M32. It is evident from these figures that significant FUV and NUV

¹ Observatories of the Carnegie Institution of Washington, 813 Santa Barbara St., Pasadena, CA 91101; agpaz, barry@ociw.edu

² Center for Space Astrophysics, Yonsei University, Seoul 120-749, Korea; sohnjy, ywlee, byun@csa.yonsei.ac.kr

³ California Institute of Technology, MC 405-47, 1200 East California Boulevard, Pasadena, CA 91125; mseibert, tab, krl, friedman, cmartin, patrick, ds, tas, wyder@srl.caltech.edu

⁴ Department of Physics and Astronomy, University of California, Los Angeles, CA 90095; rmr@astro.ucla.edu

⁵ Center for Astrophysical Sciences, The Johns Hopkins University, 3400 N. Charles St., Baltimore, MD 21218; bianchi@skysrv.pha.jhu.edu

⁶ Laboratoire d’Astrophysique de Marseille, BP 8, Traverse du Siphon, 13376 Marseille Cedex 12, France; jose.donas, roger.malina, bruno.milliard@astrsp-mrs.fr

⁷ Department of Physics and Astronomy, The Johns Hopkins University, Homewood Campus, Baltimore, MD 21218; heckman, szalay@pha.jhu.edu

⁸ Space Sciences Laboratory, University of California at Berkeley, 601 Campbell Hall, Berkeley, CA 94720; patj, ossy, bwelsh@ssl.berkeley.edu

⁹ Laboratory for Astronomy and Solar Physics, NASA Goddard Space Flight Center, Greenbelt, MD 20771; neff@stars.gsfc.nasa.gov

emission from the disk of M31 seriously affects M32 and that it is complex with a steep NW-SE gradient. The average FUV (NUV) background associated with the disk of M31 that we measure close to the position of M32 is 26.0 (25.7) mag arcsec $^{-2}$, while the background observed far from the disk of M31 is much lower, 27.2 (26.7) mag arcsec $^{-2}$. Therefore, if we want to derive reliable surface photometry for M32, detailed modeling of the M31 disk emission is required.

Finally, we complemented our GALEX observations with archival *HST* data obtained with the STIS FUV MAMA (G0 9053; PI: T.M. Brown). The *HST* image allows us to analyze the innermost $16''$ (in radius) of M32 at high spatial resolution ($<0.1''$).

3. ANALYSIS

3.1. Subtraction of the Disk of M31

The morphology of the disk of M31 both in the FUV and NUV is very clumpy (see Figures 1a & 1b), mostly due to the distinct contribution of OB associations and HII regions. This makes the modelling of the disk more complicated than at optical wavelengths where the light distribution is significantly smoother and can be reasonably well reproduced by an exponential disk (Peletier 1993; Choi et al. 2002).

The subtraction of the disk of M31 was carried out in two steps. First, we removed the unresolved, diffuse background component. For the purpose of modeling this background component we masked all the individual clusters, associations, field stars, and M32 itself. Then, we divided the image into boxes of $75'' \times 75''$ and fitted a low-order polynomial to the remaining (un-masked) pixels using the IRAF task SURFIT. We then subtracted the fitted background from the images and added the mean value of the modelled sky.

In the second step of subtracting the M31 disk, we removed the point-sources contribution by modelling the PSF of the GALEX images using the IRAF task PSF. We then subtracted the point sources previously identified by DAOFIND using the task SUBSTAR.

The final result from the subtraction of both the unresolved background and point sources is shown in Figures 1c & 1d for the FUV and NUV images, respectively. A few point sources in the outer regions of the halo of M32 and residuals from the point-source subtraction were further masked in order to derive the surface brightness and color profiles of M32.

3.2. Surface Brightness and Color Profiles

To compute the FUV and NUV surface brightness profiles of M32 we used isophotal parameters derived by both Peletier (1993) and Choi et al. (2002) at optical wavelengths. This allowed us to directly compare our UV surface photometry with that derived in the optical and obtain self-consistent UV-optical color profiles. Note that in both of the above papers the contamination from the disk of M31 was explicitly accounted for. For sake of comparison we also fitted isophotes to our final NUV image using the iterative method of Jedrzejewski (1987). We found very small differences both in ellipticity (-0.04 ± 0.04) and position angle ($2 \pm 6^\circ$) between our best-fitting isophotes and those of Peletier (1993).

In Figure 2 we show the FUV and NUV surface brightness profiles (in AB magnitudes) obtained from GALEX observations. The equivalent isophotal radius in this plot is computed as $\sqrt{a \times b}$. The *B*-band and UIT FUV surface brightness profiles published by Peletier (1993) and Ohl et al. (1998), respectively, are also plotted for comparison.

The best-fitting Sérsic-law indices of the FUV and NUV surface brightness profiles shown in Figure 2 are 0.38 ± 0.01 and 0.26 ± 0.01 , respectively. These values are very similar to what is expected for a pure de Vaucouleurs profile (0.25). Note that our UV observations do not reach the larger galactocentric distances where Graham (2002) reported the presence of an extended exponential disk.

For the innermost regions of the FUV surface brightness profile of M32 we have used an archival *HST*-STIS image. The background was estimated by matching the outermost part of the *HST* profile (obtained using ground-based optical isophotal parameters) with the GALEX FUV profile (see Figure 2).

As seen in Figure 3a all the color gradients obtained are rather flat within an r_{eff} ($32''$; e.g. Choi et al. 2002). Optical data used in this plot come from Peletier (1993); however almost identical results are obtained if data from Choi et al. (2002) are used. It is noteworthy that this behavior is observed even at distances as close to the galaxy center as $2''$, below which atmospheric seeing starts to affect ground-based optical photometry (see Figure 3b).

4. DISCUSSION

4.1. M32 and the Origin of the UV-upturn

A least-squares fit to the (*FUV*–*B*) color profile between $6''$ (FWHM) and $32''$ (r_{eff}) in radius yields a color gradient of $\Delta(FUV-B)/\Delta \log(r) = +0.15 \pm 0.03$ (see Figure 3b). This value is similar to that obtained by Ohl et al. (1998) for luminous elliptical galaxies ($+0.5 \pm 0.3$), but it is very different from that obtained for M32 by Ohl et al. (1998) ($\Delta(FUV-B)/\Delta \log(r) < -2$). First, we checked whether the difference found arises from the UIT surface photometry obtained by Ohl et al. (1998) being significantly affected by the emission of the disk of M31. To check this we derived the same (*FUV*–*B*) color gradient using the background subtraction procedure described above on the archival Astro-1 (B1 filter; $\lambda_{\text{eff}} = 1520 \text{ \AA}$) FUV UIT image. The color profile obtained is remarkably similar to that obtained by Ohl et al. (1998) (see Figure 3b) after being offset to match the Astro-2 (B5 filter; $\lambda_{\text{eff}} = 1615 \text{ \AA}$) FUV UIT photometry. We also studied the effects of the wings of the UIT PSF on the (*FUV*–*B*) profile. The maximum impact of this effect on the (*FUV*–*B*) color gradient is found to be $\leq 0.4 \text{ mag}$ within the central $30''$. The other possibility is that this difference may be a problem in the density-to-flux calibration of the (photographic) UIT image at very low surface-brightness levels. However, a detailed study of the linearity of the UIT data is beyond the scope of this Letter.

The GALEX (*FUV*–*NUV*) color gradient (also sensitive to the strength of the UV-upturn) is similar to that derived for (*FUV*–*B*). This confirms that the color gradient derived is real and not an artifact introduced by the different background-subtraction technique or because of spatial resolution differences between the UV and optical

data. This is confirmed by the analysis of the archival *HST*-STIS data, which shows a gradient at the innermost regions of the galaxy similar to and extending that obtained from GALEX observations alone (see Figure 3b).

Despite its very shallow UV-upturn, which in principle could be explained by emission from post-AGB stars, Brown et al. (2000) have shown that the UV emission in M32 is dominated by hot HB stars. By analogy, this suggests that hot HB stars are also responsible for most of the FUV emission associated with the UV-upturn observed in luminous elliptical galaxies (see Brown et al. 1997). The $(FUV-B)$ color gradient reported in this Letter, similar to that measured in luminous elliptical galaxies, along with the results of Brown et al. (2000) suggest that the properties and spatial distribution of the hot HB stars in M32 are the same as those in luminous elliptical galaxies. The great advantage here being that M32 is the only object where individual hot-HB stars have actually been resolved.

Burstein et al. (1988) claimed that elliptical galaxies with larger Mg_2 indices show stronger UV-upturns. This has been interpreted as resulting from a dependence of mass-loss efficiency and helium abundance on metallicity (Greggio & Renzini 1990; O’Connell 1999). However, Rich et al. (2004), using a large sample of low-redshift red galaxies, do not find any correlation between the strength of the UV-upturn and the Mg_2 , D4000, $H\beta$ indices or the velocity dispersion (see also Deharveng, Boselli, & Donas 2002). Ohl et al. (1998) also reported a lack of correlation between the $(FUV-B)$ gradient and the Mg_2 -index gradient. These results suggest the presence of a second parameter (decoupling from the Fe-peak, helium abundance, age; O’Connell 1999) that could have an impact even stronger than the metallicity on the evolution of the UV-upturn.

The suggested presence of a strong negative gradient in $(FUV-B)$ color in M32 (Ohl et al. 1998), where the existence of an intermediate age stellar population (spatially segregated toward the galaxy center) has been frequently proposed (Grillmair et al. 1996), had been claimed as an indication that the age may play a significant role in the evolution of the UV-upturn. However, our results in combination with the lack of structure in the optical-colors and spectroscopic-index maps of M32 (e.g. del Burgo et al. 2001) indicate that if this stellar population is present, it

is very smoothly distributed across the body of the galaxy and that the properties of the hot HB responsible for the UV-upturn are also very similar at any position in the galaxy.

4.2. Is M32 a Peculiar Object?

The two most intriguing differences reported between the properties of M32 and those of luminous elliptical galaxies had been: (1) the presence of an intermediate-aged stellar population (e.g. Grillmair et al. 1996) and (2) the large (inverted) $(FUV-B)$ color measured by Ohl et al. (1998). Regarding the former problem we note that many of the spectral synthesis analyses carried out to date assume a pure red clump HB morphology, while Brown et al. (2000) have identified a large population of hot HB stars in M32. With regard to the latter topic, our results show that the previously reported unusual $(FUV-B)$ color gradient does not exist and that the UV properties of M32 are very similar to those of luminous ellipticals.

We conclude that, although M32 is certainly an extreme example in the sequence of elliptical galaxies in many of its properties and the possible presence of an intermediate-aged stellar population should not be ignored, it cannot be considered to be a peculiar object and its use as a reference object for stellar populations synthesis is justified.

In summary, the analysis of GALEX FUV and NUV imaging data of the compact elliptical galaxy M32 yields very small (positive) $(FUV-B)$ and $(FUV-NUV)$ color gradients, comparable to values seen in luminous elliptical galaxies. This result suggests that the properties of the hot HB stars responsible for the formation of the (very weak) UV-upturn in M32 are not a strong function of position in the galaxy and that they are probably similar to hot HB stars in luminous elliptical galaxies.

GALEX (Galaxy Evolution Explorer) is a NASA Small Explorer, launched in April 2003. We gratefully acknowledge NASA’s support for construction, operation, and science analysis for the GALEX mission, developed in co-operation with the Centre National d’Etudes Spatiales of France and the Korean Ministry of Science and Technology. We thank Robert W. O’Connell and Jean-Michel Deharveng for valuable comments.

REFERENCES

- Brown, T. M., Ferguson, H. C., Davidsen, A. F., & Dorman, B. 1997, *ApJ*, 482, 685
 Brown, T. M., Bowers, C. W., Kimble, R. A., Sweigart, A. V., & Ferguson H. C. 2000, *ApJ*, 532, 308
 Burnstein, D., Bertola, F., Buson, L. M., Faber, S. M., & Lauer, T. R. 1988, *ApJ*, 328, 440
 Choi, P. I., Guhathakurta, P., & Johnston, K. V. 2002, *AJ*, 124, 310
 Deharveng, J.-M., Boselli, A., & Donas, J. 2002, *A&A*, 393, 843
 del Burgo, C., Peletier, R. F., Vazdekis, A., Arribas, S., & Mediavilla, E. 2001, *MNRAS*, 321, 227
 Freedman, W. L. 1992, *AJ*, 104, 1349
 Freedman, W. L., & Madore, B. F. 1990, *ApJ*, 365, 186
 Graham, A. W. 2002, *ApJ*, 568, L13
 Greggio, L., & Renzini, A. 1990, *ApJ*, 364, 35
 Grillmair, C. J., et al. 1996, *AJ*, 112, 1975
 Jedrzejewski, R. I., 1987, *MNRAS*, 226, 747
 Morrissey, P., et al. 2004, *ApJ*, present volume.
 O’Connell, R. W. 1999, *ARA&A*, 37, 603
 O’Connell, R. W., et al. 1992, *ApJ*, 395, L45
 Ohl, R. G., et al. 1998, *ApJ*, 505, L11
 Peletier, R. F. 1993, *A&A*, 271, 51
 Rich, R. M., et al. 2004, *ApJ*, present volume.
 Tonry, J. L. 1991, *ApJ*, 373, L1

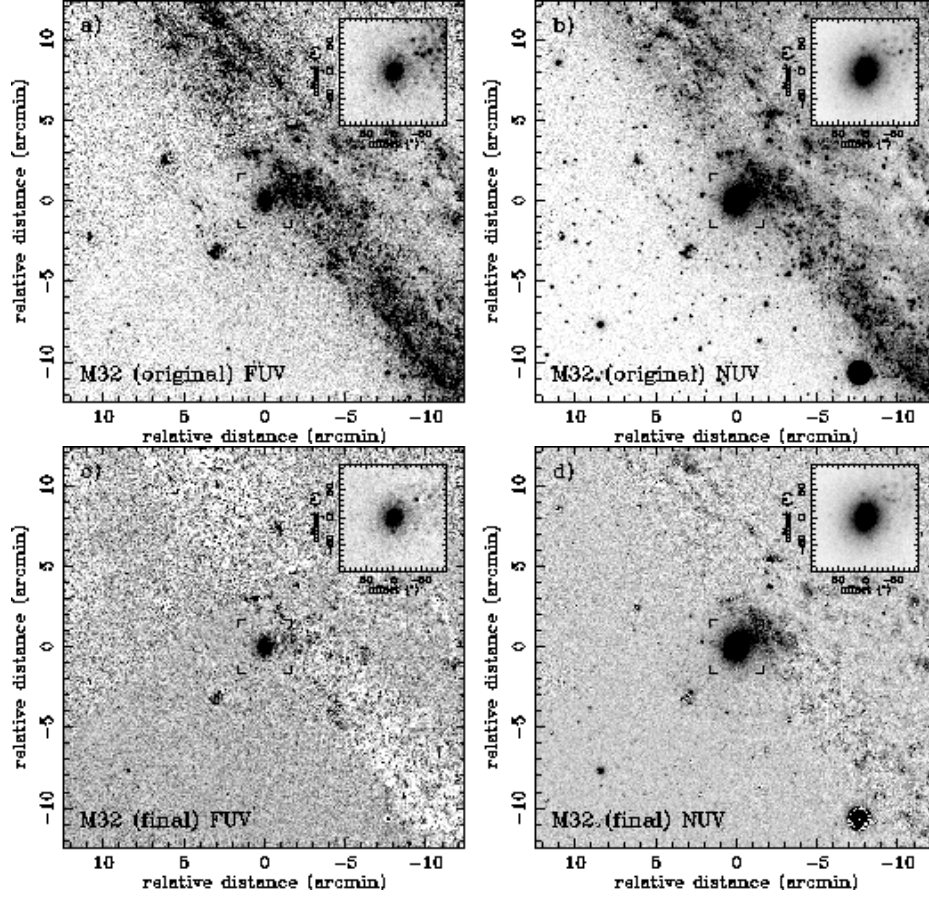


FIG. 1.— GALEX UV images of M32. **a)** Combined GALEX FUV image corresponding to a total exposure time of 6138 seconds at the position of M32. A $2\times$ expanded view centered on M32 is shown in the upper-right corner of each plot (with a different stretch). **b)** The same as **a** for the NUV channel. The total exposure time at the position of M32 for this image was 4808 seconds. **c)** GALEX FUV image after the subtraction of point sources and the unresolved background from M31. **d)** The same as **c** for the NUV channel.

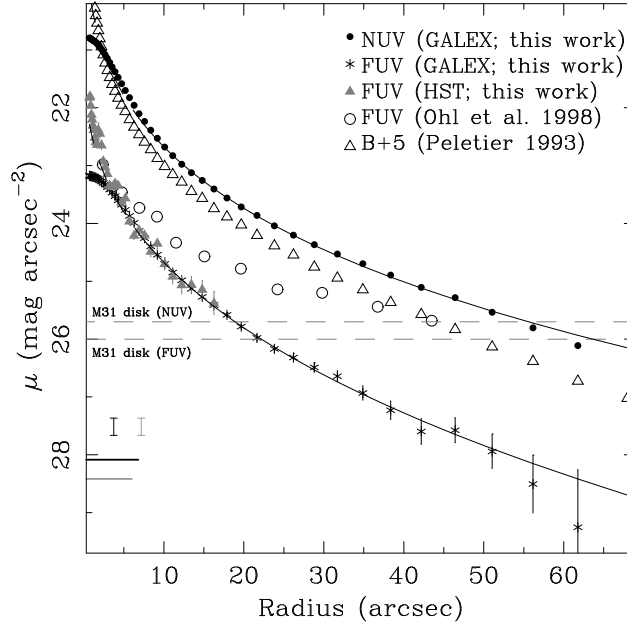


FIG. 2.— Surface brightness profiles of M32. The surface brightness profiles of M32 in the GALEX FUV, NUV, and optical B bands are shown (we have adopted the isophotal parameters derived by Peletier 1993). The best-fitting Sérsic laws for the FUV and NUV profiles are also shown. The FUV surface photometry published by Ohl et al. (1998) is shown as open circles in this plot. Grey triangles indicate the FUV surface brightness profile obtained from archival *HST*-STIS data. The absolute calibration errors of 0.15 mag and the PSF FWHM of the FUV and NUV images are shown in the lower-left corner of the plot using grey and black tick marks, respectively. The horizontal broken lines are the approximate levels of the M31 background contamination at the position of M32 in the FUV and NUV bands.

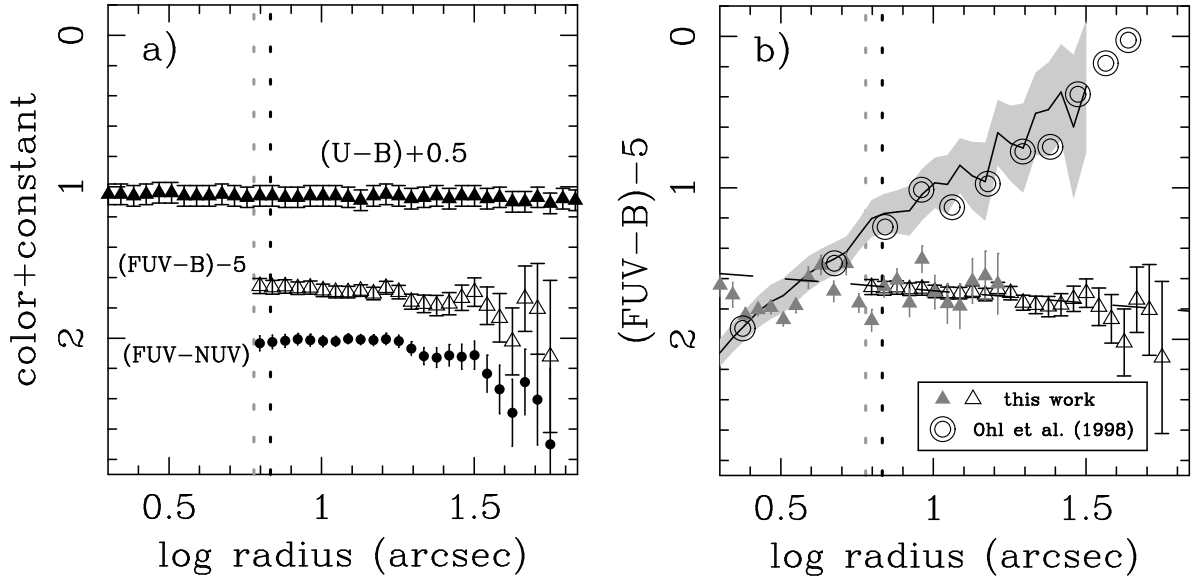


FIG. 3.— Color profiles of M32. **a)** $(U-B)$, $(FUV-B)$, and $(FUV-NUV)$ color profiles of M32. Optical data have been taken from Peletier (1993). Vertical grey and black broken lines show the position of the PSF FWHM of the FUV and NUV images, respectively. **b)** $(FUV-B)$ color profile obtained by GALEX (open triangles) compared with that obtained using the published FUV photometry data of Ohl et al. (1998) (circled circles). The black solid curve and the grey-shaded areas show the mean and $\pm 1-\sigma$ color profile obtained by us using the same background subtraction procedure for the GALEX data described in the body of this Letter, but applied to the UIT image. The best-fitting $(FUV-B)$ color gradient to the GALEX data (not including the *HST*-STIS data) is also shown as a broken line. Grey triangles show the color profile of the innermost 16'' of M32 obtained from *HST*-STIS FUV and ground-based *B*-band photometry.